International Immunopharmacology 143 (2024) 113441

Contents lists available at ScienceDirect

International Immunopharmacology

journal homepage: www.elsevier.com/locate/intimp

# CD36 deficiency protects lipopolysaccharide-induced sepsis via inhibiting CerS6-mediated endoplasmic reticulum stress

Min Hee Kim [a,1], Hyomin Lim [a,1], Ok-Hee Kim [b,c], Byung-Chul Oh [b,c], YunJae Jung [c,d], Kyung-Ha Ryu [e], Joo-Won Park [a,*], Woo-Jae Park [f,*]

[a] Department of Biochemistry, College of Medicine, Ewha Womans University, Seoul 07084, Republic of Korea
[b] Department of Physiology, College of Medicine, Gachon University, Incheon 21999, Republic of Korea
[c] Department of Health Sciences and Technology, GAIHST, Gachon University, Incheon 21999, Republic of Korea
[d] Department of Microbiology, College of Medicine, Gachon University, Incheon 21999, Republic of Korea
[e] Department of Pediatrics, College of Medicine, Ewha Womans University, Seoul 07804, Republic of Korea
[f] Department of Biochemistry, Chung-Ang University College of Medicine, Seoul 06974, Republic of Korea

ARTICLE INFO

*Keywords:*
Ceramide synthase 6
Acyl chain length
Inflammasome
CD36
Endoplasmic reticulum stress

ABSTRACT

The type 2 scavenger receptor CD36 functions not only as a long chain fatty acid transporter, but also as a pro-inflammatory mediator. Ceramide is the simple *N*-acylated form of sphingosine and exerts distinct biological activity depending on its acyl chain length. Six ceramide synthases (CerS) in mammals determine the chain length of ceramide species, and CerS6 mainly produces C16-ceramide. Endotoxin-induced septic shock shows high mortality, but the pathophysiologic role of sphingolipids involved in this process has been hardly investigated. This paper aims to highlight the different role of CerS isoforms in endotoxin-induced inflammatory responses and the regulatory role of CD36 in CerS6 protein degradation with an emphasis as the potential therapeutic candidates in humans. Lipopolysaccharide (LPS), the endotoxin of the Gram-negative bacterial cell wall, was treated to induce endotoxin-induced inflammation both *in vitro* and *in vivo*. CerS6-derived C16-ceramide propagated LPS-induced inflammatory responses activating various intracellular signaling pathways, such as mitogen-activated protein kinase and nuclear factor-κB, resulting in the formation of inflammasome complex and pro-inflammatory cytokines. Mechanistically, CerS6-derived C16-ceramide augmented inflammatory responses via endoplasmic reticulum stress, and CerS6 protein stability was regulated by CD36. Finally, CerS6 protein expression and LPS-induced lethality were strikingly reduced in CD36 knockout mice. Collectively, our findings show that CerS6-derived C16-ceramide plays a pivotal role in endotoxin-induced inflammation and suggest CerS6 and its regulator CD36 as possible targets for therapy under life-threatening inflammation such as septic shock.

## 1. Introduction

Sepsis is defined as multi-organ dysfunction induced by aberrant or dysregulated host response to infection [1]. Systemic inflammation, eventually causing multi-organ failure, is accompanied by sepsis, and overwhelming inflammation is linked to higher mortality rates [2,3]. Lipopolysaccharide (LPS), a major component of the outer membrane of Gram-negative bacteria, is a potent endotoxin responsible for sepsis or septic shock [4], and macrophages are regarded as the main producers of pro-inflammatory cytokines following administration of LPS in experimental animals [5]. Macrophages reside in all the tissues and contribute to the removal of damaged cells or bacteria by phagocytosis, thus playing a pivotal role in tissue homeostasis as well as innate immunity. LPS interaction with Toll-like receptor 4 (TLR4) instigates intracellular signaling cascades, such as mitogen-activated protein (MAP) kinases and nuclear factor-κB (NF-κB), eventually leading to the production of pro-inflammatory cytokines and inflammasome.

Sphingolipids (SLs) have recently emerged not only as key mediators in the inflammatory process but also as pivotal drug targets, together with associated enzymes and receptors, for the treatment of pathological inflammation [6]. *De novo* synthesis of ceramide, which is central for SL metabolism, is initiated by the condensation of palmitoyl CoA and L-

* Corresponding authors.
*E-mail addresses:* joowon.park@ewha.ac.kr (J.-W. Park), ooze@cau.ac.kr (W.-J. Park).
[1] Contributed equally to this manuscript.

https://doi.org/10.1016/j.intimp.2024.113441
Received 2 September 2024; Received in revised form 15 October 2024; Accepted 17 October 2024
Available online 25 October 2024

**Table 1**
Primers used for real-time PCR.

| Gene | Primer sequences |
|---|---|
| *CerS1* (mouse) | F: 5′-TCCATCTATGCCACCGTGTA-3′<br>R: 5′-GCGTAGGAAGAGGCAATGAG-3′ |
| *CerS2* (mouse) | F: 5′-TCTGCATGACGCTTCTGACT-3′<br>R: 5′-GATGGCGAACACAATGAAGA-3′ |
| *CerS3* (mouse) | F: 5′-AAGCATTCCACAAGCAAACC-3′<br>R: 5′-GCCGAATCCTAAGCCATCTT-3′ |
| *CerS4* (mouse) | F: 5′-TGCGCATGCTCTACAGTTTC-3′<br>R: 5′-CAGAAACTGGCTCGTCATCA-3′ |
| *CerS5*(mouse) | F: 5′-GCAATCTTCCCATTGTGGAT-3′<br>R: 5′-TCAGGAGAAGGGCATTGAAG-3′ |
| *CerS6* (mouse) | F: 5′-TTAGCTACGGAGTCCGGTTC-3′<br>R: 5′-TGAAGGTCAGCTGTGAGTGG-3′ |
| *GAPDH* (mouse) | F: 5′-ACTCACGGCAAATTCAACGG-3′<br>R: 5′-ATGTTAGTGGGGTCTCGCTC 3′ |

serine to 3-ketosphinganine, which is further reduced to sphinganine by 3-ketosphinganine reductase. Sphinganine is acylated by ceramide synthase (CerS) to produce dihydroceramide, which is finally reduced to ceramide by dihydroceramide reductase [7,8]. In mammals, a family of six CerS (CerS1−6) attaches acyl-CoAs of defined chain length to sphinganine [9]. CerS1 and CerS2 form C18- and C22−24-ceramide, respectively. CerS3 generates the longest form of ceramide with a chain length longer than C26-ceramide. CerS4 mainly synthesizes C20-ceramide, while both CerS5 and CerS6 generate C16-ceramide in common. A significant body of research reported a distinct role of ceramides depending on their acyl chain length in a variety of cellular events, such as proliferation, cell death, migration, oxidative stress, and immune reaction. CerS2- and CerS6-deficient mice showed opposite phenotypes in the same model of experimental autoimmune encephalomyelitis [10,11], implicating the chain length of ceramides as a possible influence on neutrophil function. Similarly, the protective role of CerS2 and the detrimental role of CerS6 have been previously reported in palmitate-induced endoplasmic reticulum (ER) stress and fatty liver disease [12]. Furthermore, a shift in SL composition from C24 to C16 increased cisplatin-induced apoptosis in HeLa cells [13]. Considering the different roles of each CerS and its derivatives in various pathogenic mechanisms, the current study was designed to validate the effects of ceramide chain length on LPS-induced inflammation in macrophages.

Beside SLs, long-chain saturated fatty acids are thought to exert a pro-inflammatory role via activating TLR4 signaling [14]. CD36 is a class B scavenger receptor expressed on the surface of a variety of cells, and one of its major roles is to facilitate fatty acid uptake by functioning as a fatty acid transporter [15]. CD36 also regulates the metabolism and functions of immune cells, including macrophages, and participates in the activation of the inflammasome pathways [15]. In addition, CD36 expression has also been shown to influence NF-κB signaling and inflammatory cytokine production in primary goat mammary epithelial cells exposed to LPS [16]. Furthermore, CD36-deficient mice were protected from antibiotic-treated cecal ligation and puncture-induced sepsis [17]. Given this evidence for a pro-inflammatory role of CD36, this study aims to examine a role of CD36 in LPS-induced inflammation and to investigate the potential mechanistic role of CerS and its derivative SL species in this process. The present study recognizes potential relationships between SL and fatty acid metabolism and extends functional knowledge of multicomponent lipid metabolism. This study would ultimately provide potential therapeutic candidates against uncontrolled inflammation such as sepsis.

## 2. Material and methods

### 2.1. Materials

The materials were purchased as follows: 1) LPS, palmitate, thapsigargin, 4-phenylbutyric acid (4-PBA), tauroursodeoxycholic acid (TUDCA), sulfo-*N*-hydroxysuccinimidyl ester of oleate (SSO), anti-CerS2 antibody (HPA027262), and anti-α-tubulin antibody (T9026) (Sigma-Aldrich, St. Louis, MO); 2) anti-TLR4 (14358), anti-inducible nitric oxide synthase (anti-iNOS; 13120), anti-phospho-p65 (3033), anti-phospho-IκB (2859), anti-phospho-p38 (4511), anti-phospho-c-Jun N-terminal kinase (anti-p-JNK; 9255), anti-phospho-extracellular signal-regulated kinase (anti-p-ERK; 4370), anti-phospho-protein kinase R-like endoplasmic reticulum kinase (anti-p-PERK; 3179), anti-phospho-eukaryotic initiation factor-2α (anti-p-eIF2α; 3597), anti-ubiquitin (3936), and anti-NOD-like receptor protein 3 (anti-NLRP3; 15101) antibodies (Cell Signaling Technology, Beverly, MA); 3) anti-CD36 (sc-7309), anti-CerS6 (sc-100554), anti-caspase1 (sc-56036), and anti-apoptosis-associated speck-like protein containing a caspase recruitment domain (anti-ASC; sc-22514-R) antibodies (Santa Cruz Biotechnology, Dallas, TX); 4) anti-CerS1 antibody (H00010715-M01; Abnova, Taipei, Taiwan); 5) anti-glyceraldehyde 3-phosphate dehydrogenase (anti-GAPDH) antibody (MAB374; EMD Millipore, Billerica, MA); 6) interleukin (IL)-1β antibody (NB600-633) (Novus Biologicals, Littleton, CO); and 7) anti-mouse-horseradish peroxidase (anti-mouse-HRP; 115–036-003) and anti-rabbit-HRP (111–035-003) antibodies (Jackson Laboratory, Bar Harbor, ME).

### 2.2. Mice

CD36 knockout (KO) mice (B6.129S1-Cd36$^{tm1Mfe}$/J) were from Jackson Laboratory and maintained under specific pathogen-free conditions on a 12 h light/dark cycle with free access to food and water. Experimental procedures were approved by the Institutional Animal Care and Use Committee at Lee Gil Ya Cancer and Diabetes Institutes in Gachon University (LCDI-2021–0128), and all the experiments were carried out in accordance with the approved guidelines and regulations. To induce the sepsis model using LPS, 8-week-old male mice were intraperitoneally (i.p.) injected with LPS (20 mg/kg). To calculate the overall survival rate, mice were observed for 96 h. To harvest organs and blood, mice were euthanized with $CO_2$ inhalation 12 h after LPS injection (20 mg/kg, i.p.).

### 2.3. Lps-induced inflammatory response in macrophages

Peritoneal macrophages were collected by peritoneal lavage 4 days after 4 % thioglycolate (1 ml; Sigma-Aldrich). After centrifugation at 400 × *g* for 10 min at 4 °C, pelleted cells were suspended in Dulbecco's modified Eagle medium (DMEM; Hyclone, Logan, UT, USA) supplemented with 10 % heat-inactivated fetal bovine serum (FBS; Hyclone) and 1 % penicillin/streptomycin (P/S; Hyclone). Isolated peritoneal macrophages were stimulated with 1 μg/mL of LPS for 6 h and collected for Western blotting (WB). The RAW264.7 mouse macrophage cells were purchased from the American Type Culture Collection (ATTC, Manassas, VA) and grown in DMEM supplemented with 10 % FBS and 1 % P/S. LPS at 50 ng/mL (low dose) or 1 μg/mL (high dose) was used to induce inflammation, as previously described [18–20].

### 2.4. Transfection

RAW264.7 cells were transfected with pcDNA3.1-CerS1-HA, pcDNA3.1-CerS5-HA, pcDNA3.1-CerS6-HA, pSUPER-shCerS6, pcDNA6-CD36, or pcDNA6-TLR4 using metafectene (Biontex Laboratories GmbH, Munich, Germany) according to the manufacturer's protocol. pcDNA3.1-CerS1-HA, pcDNA3.1-CerS5-HA, pcDNA3.1-CerS6-HA, and pSUPER-shCerS6 were kindly provided by Professor Anthony H. Futerman (Weizmann Institute of Science, Rehovot, Israel). Scrambled siRNA (Silencer™ Select Negative Control No. 1, 4390843) and siCD36 (160081) were purchased from Thermo Fisher Scientific (Waltham, MA) and transfected with Lipofectamine™ RNAiMAX Transfection Reagent (Invitrogen, Carlsbad, CA).

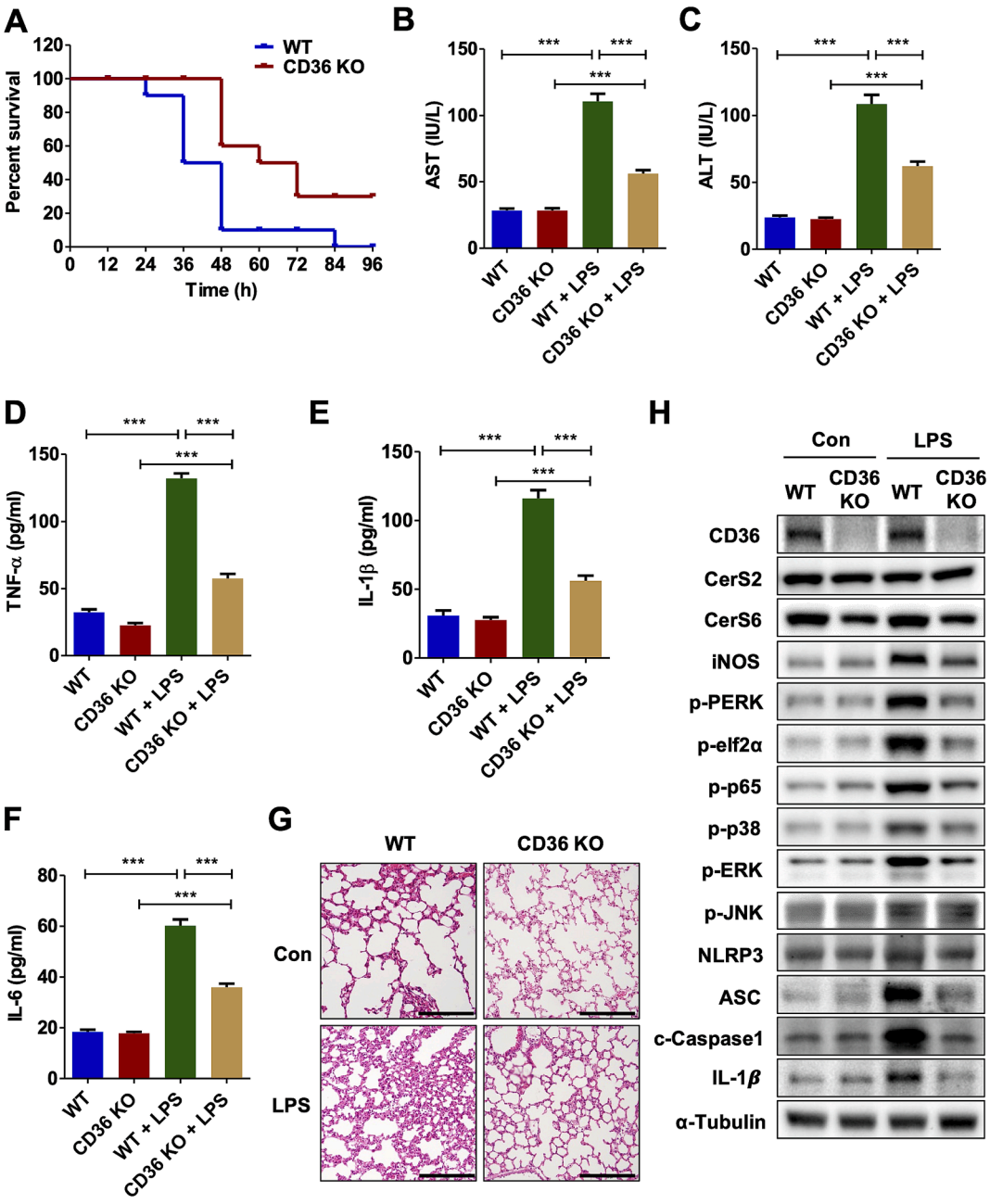


**Fig. 1. LPS-induced systemic inflammation is ameliorated in CD36 KO mice.** LPS (20 mg/kg) was intraperitoneally injected into 8-week-old male mice to induce endotoxin-induced sepsis. (**A**) Survival curve of WT and CD36 KO mice upon LPS injection ($n = 10$). Serum levels of (**B**) AST, (**C**) ALT, (**D**) TNF-α, (**E**) IL-1β, and (**F**) IL-6 with or without LPS administration in mice ($n = 10$). (**G**) H&E staining of lung sections (scale bar, 200 μm). (**H**) WB of lung tissues. The values are expressed as means ± S.E.M. ***$p < 0.001$.

### *2.5. Enzyme-linked immunosorbent assay (ELISA) and nitrite measurement*

After treating RAW264.7 cells with 50 ng/mL or 1 μg/mL of LPS for 18 h, cytokine levels of tumor necrosis factor-alpha (TNF-α), IL-1β, and IL-6 in culture medium were measured using ELISA kits (TNF-α, IL-1β, and IL-6 Mouse ELISA kits; Koma Biotech, Seoul, Republic of Korea) according to the manufacturer's indication. Nitrite in the medium was measured using Griess reagent (Sigma-Aldrich) according to the manufacturer's protocol.

### *2.6. Western blotting (WB)*

RAW264.7 or peritoneal macrophage cells were lysed using RIPA buffer (50 mM Tris-Cl, pH 7.5; 150 mM NaCl, 1 % Nonidet P-40, 0.5 % sodium deoxycholate, 0.1 % SDS, protease and phosphatase inhibitors [Sigma-Aldrich]). After centrifugation (10,000 × *g*, 10 min, 4 °C), protein levels in the supernatant were measured using Protein Assay Dye Reagent (Bio-Rad Laboratories, Hercules, CA). Fifty micrograms of proteins were separated on 8–15 % SDS-PAGE and transferred to nitrocellulose membranes (Bio-Rad Laboratories). Membranes were blocked with 5 % bovine serum albumin (BSA; Sigma-Aldrich) in TBST (TBS with 0.1 % Tween-20) for 1 h and incubated with primary antibodies overnight at 4 °C. Secondary antibodies were attached for 1 h at room temperature. Protein bands were detected by the ChemiDoc MP Imaging System (Bio-Rad Laboratories), using EzWestLumi Plus Reagents (ATTO Corp., Tokyo, Japan).

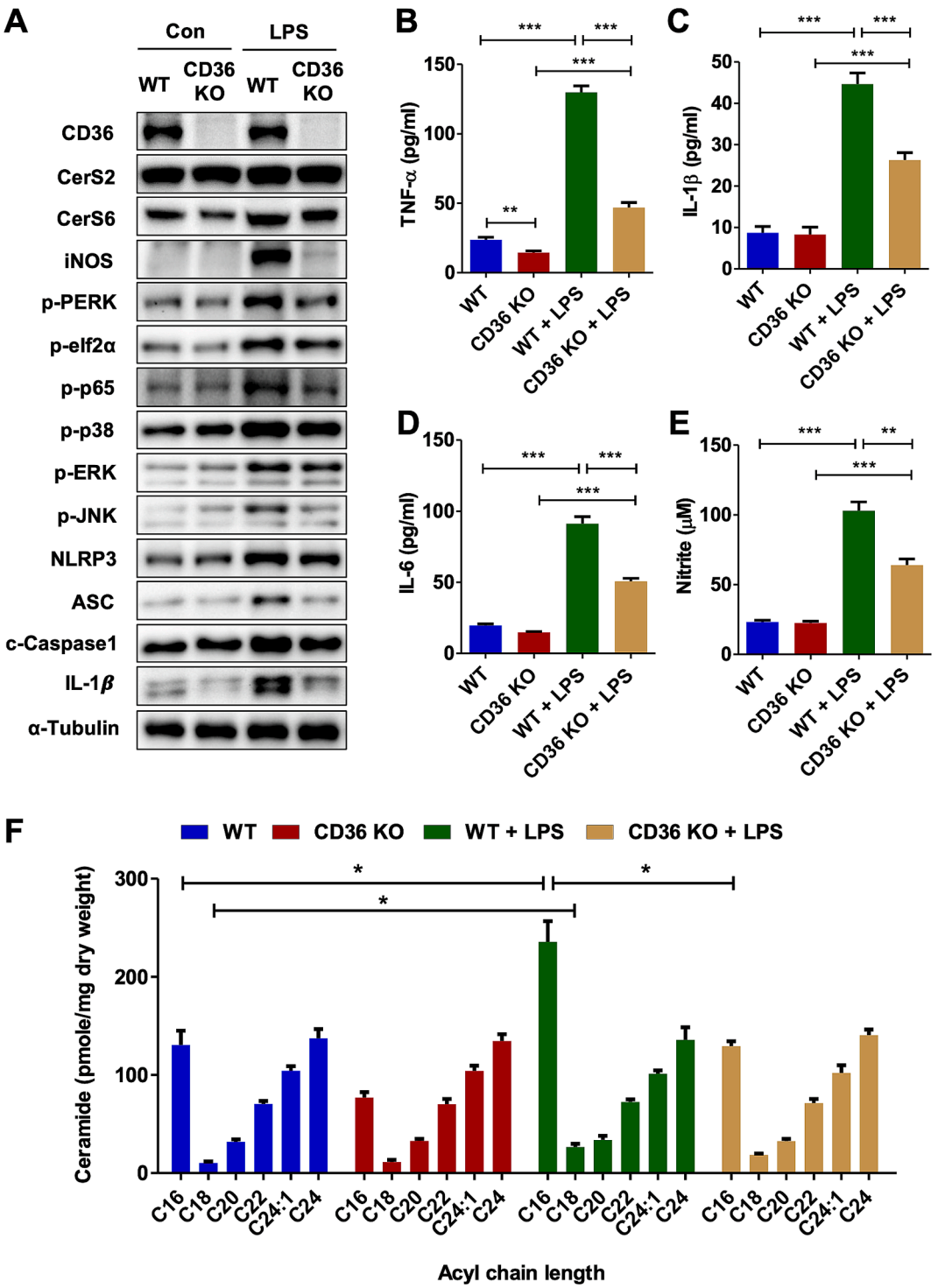


**Fig. 2. LPS-induced inflammatory response was reduced in peritoneal macrophages of CD36 KO mice compared with WT mice.** Peritoneal macrophages derived from WT or CD36 KO mice were treated with LPS (1 μg/mL). (**A**) WB of the peritoneal macrophages with or without LPS treatment (1 μg/mL, 6 h). Levels of (**B**) TNF-α, (**C**) IL-1β, (**D**) IL-6, and (**E**) nitrite in cell culture medium were measured using ELISA kits and Griess reagent ($n = 5$). (**F**) Ceramide acyl chain length of peritoneal macrophages measured by LC-ESI-MS/MS ($n = 3$). The values are expressed as means ± S.E.M. *$p < 0.05$, **$p < 0.01$, ***$p < 0.001$.

### 2.7. Real-Time PCR

After treating RAW264.7 cells with LPS (50 ng/mL or 1 μg/mL) for 18 h, total mRNA was extracted using the RNeasy Mini kit (Qiagen, Valencia, CA), and cDNA was immediately synthesized using the Verso cDNA Synthesis Kit (Thermo Scientific). Real-time PCR was performed using the SYBR Green qPCR Master Mix (Thunderbird™) in a CFX96 Real-Time PCR System (Bio-Rad). Relative gene expression was calculated using the $2^{-\Delta\Delta Ct}$ method [21]. The primers used in this study are described in Table 1.

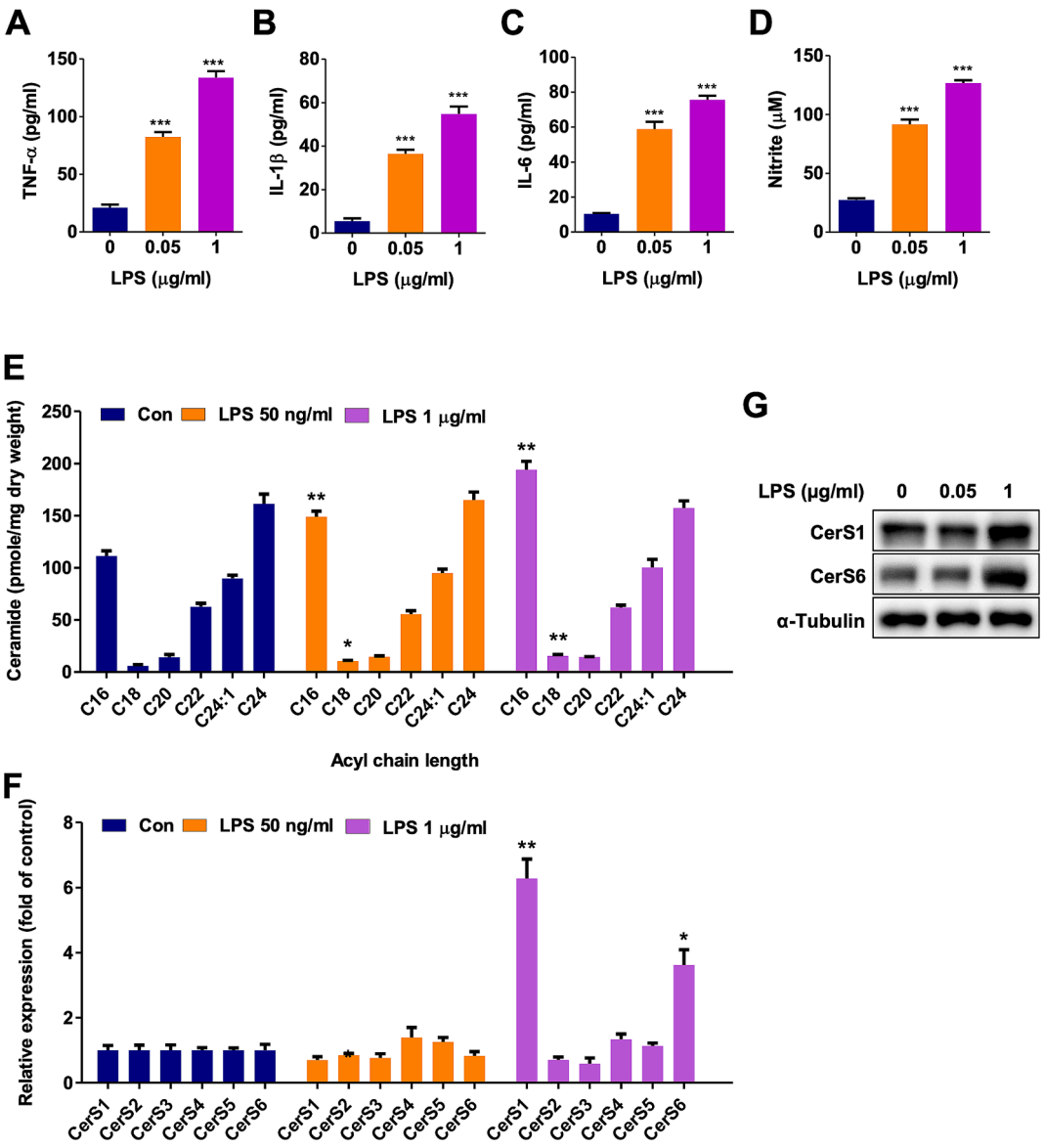


**Fig. 3. LPS dose-dependently increases C16- and C18-ceramides in RAW264.7 cells.** LPS was treated at two concentrations (50 ng/mL and 1 μg/mL) to RAW264.7 cells for 18 h. Levels of (**A**) TNF-α, (**B**) IL-1β, (**C**) IL-6, and (**D**) nitrite in cell culture medium ($n = 5$). (**E**) Ceramide acyl chain length of RAW264.7 cells measured by LC-ESI-MS/MS ($n = 3$). (**F**) Relative *CerS* mRNA levels upon LPS treatment in RAW264.7 cells ($n = 3$). (**G**) WB of RAW264.7 cells treated with LPS. The values are expressed as means ± S.E.M. $^{*}p < 0.05$, $^{**}p < 0.01$, $^{***}p < 0.001$.

### *2.8. Liquid chromatography – electrospray ionization-tandem mass spectrometry (LC-ESI-MS/MS) analysis of ceramide*

Ceramide levels were measured using LC-ESI-MS/MS, as described previously [12].

### *2.9. Measurement of aspartate transaminase (AST) and alanine transaminase (ALT)*

Serum AST and ALT levels were analyzed using a Reflotron (Roche Diagnostics, Basel, Switzerland).

### *2.10. Hematoxylin and eosin (H&E) staining*

Paraffin-embedded tissues cut at 4-μm thickness were mounted onto slides, and after hydration, the sections were stained with hematoxylin for 2 min and submerged in ethanol containing 1 % HCl. After washing, the sections were stained with eosin.

### *2.11. Cycloheximide (CHX) chase assay*

RAW264.7 cells were treated with CHX (10 μg/mL) to inhibit the synthesis of new proteins and then subjected to WB to assess protein degradation.

### *2.12. Proteasome 20S activity*

Proteasome 20S activity was measured using the Proteasome 20S Activity Assay Kit (Sigma-Aldrich) according to the manufacturer's instructions.

### *2.13. Ubiquitination assay*

RAW264.7 cells were treated with SSO (100 μM, 24 h) or siCD36 (100 nM, 48 h). Then, cell pellets were collected and lysed with lysis buffer (20 mM Tris-Cl, pH 8.0; 137 mM NaCl, 10 % glycerol, 1 % NP-40, 2 mM EDTA, protease inhibitor). Next, cell lysates were precleared with

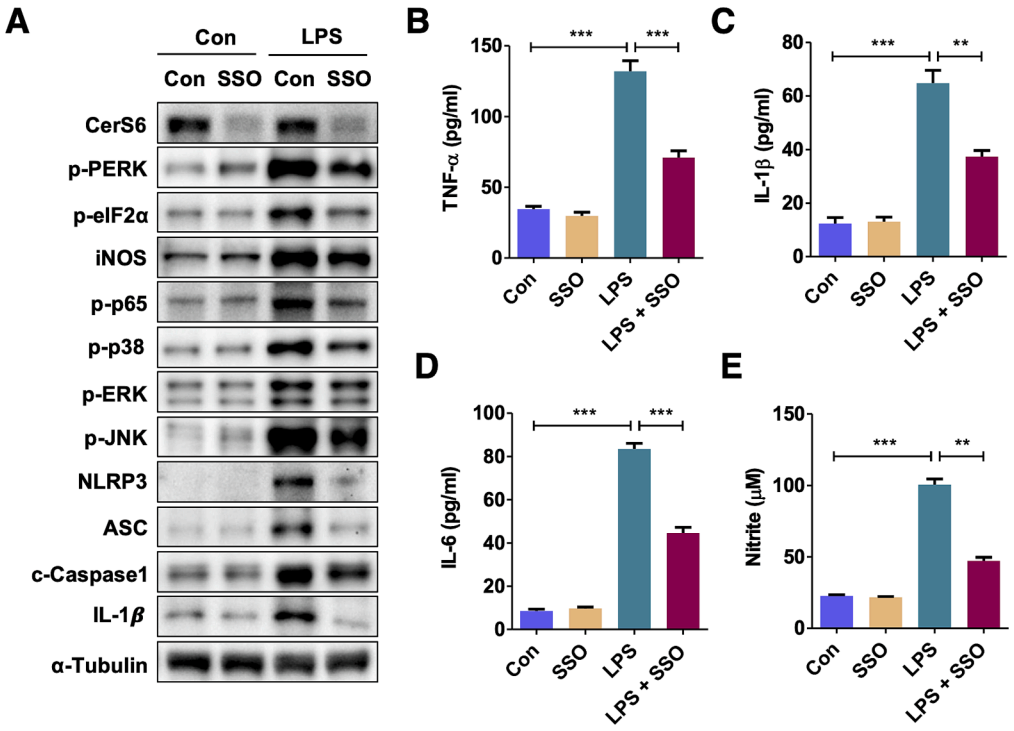


**Fig. 4. CD36 inhibition partially normalizes LPS-induced inflammatory response with concomitant decrease of CerS6 protein expression.** (**A**) WB of RAW264.7 cells with combinational treatment of LPS (50 ng/mL, 18 h) and SSO (100 μM, 30 h). Levels of (**B**) TNF-α, (**C**) IL-1β, (**D**) IL-6, and (**E**) nitrite were measured in RAW264.7 cell culture medium using ELISA kits and Griess reagent ($n = 5$). The values are expressed as means ± S.E.M. $^{**}p < 0.01$, $^{***}p < 0.001$.

Protein A/G Plus-Agarose beads (Santa Cruz Biotechnology) for 1 h on a rotator at 4 ℃. Cell lysates were then incubated with CerS6 antibody for 18 h, followed by Protein A/G Plus-Agarose beads for another 2 h on a rotator at 4 ℃. The gel beads were washed four times with lysis buffer, resuspended in 2X sample buffer, and analyzed with immunoblotting using indicated antibodies.

### 2.14. Statistical analyses

All the experiments were repeated at least three times independently, and values are given as the mean ± standard error of the mean (S.E.M.). Statistical significance was calculated using ANOVA or two-tailed Student's *t*-test with Prism 7 software (GraphPad Software, Inc., San Diego, CA). A *p*-value of $< 0.05$ was considered statistically significant ($^{***}p < 0.001$; $^{**}p < 0.01$; $^{*}p < 0.05$).

## 3. Results

### 3.1. Response to LPS-induced sepsis is alleviated by CD36 deficiency

To investigate the impact of CD36 on LPS-induced inflammation and to reveal the potential mechanistic role of CerS in this process, LPS-induced sepsis model was applied to wild-type (WT) and CD36 KO mice. Similar to cecal ligation and puncture-induced sepsis data [17], CD36 deficiency improved survival in the LPS-induced sepsis model (Fig. 1A). Serum AST and ALT levels were markedly increased by LPS treatment in WT mice, while they were partially restored in CD36 KO mice (Fig. 1B and C), indicating the protective effect of CD36 deficiency on sepsis-associated liver damage. Plasma levels of pro-inflammatory cytokines, such as TNF-α (Fig. 1D), IL-1β (Fig. 1E), and IL-6 (Fig. 1F), elevated by LPS administration in WT mice were also significantly diminished in CD36 KO mice, implicating that LPS-induced systemic inflammation is alleviated in CD36 KO mice.

LPS treatment also induced destruction of lung structure and infiltration of immune cells in WT lung, whereas lung architecture in CD36 KO mice was relatively preserved with only mild histopathological changes (Fig. 1G). In accordance with lung histology (Fig. 1G), ER stress (PERK/eIF2α phosphorylation), iNOS, NF-κB (p65 phosphorylation), MAP kinase (p38/ERK/JNK phosphorylation), and NLRP3 inflammasome (NLRP3/ASC/Caspase-1) signaling cascades were induced by LPS in WT lung, resulting in the production of pro-inflammatory cytokine IL-1β, while activation of these signaling pathways was markedly reduced in LPS-treated CD36 KO lung (Fig. 1H). Ceramides with different acyl chain lengths, generated by CerS2 and CerS6, modulate the ER stress response [12]; therefore, we examined whether CD36 deficiency is related to altered CerS2 or CerS6 levels. Interestingly, CerS6 protein levels were markedly reduced in CD36 KO lung (Fig. 1H). Similarly, CerS6 protein levels were also reduced in the liver, skeletal muscle, and gonadal white adipose tissue of CD36 KO mice (Supplementary Fig. S1A). CerS2 protein expression was not altered in CD36 KO mice except for an elevation in white adipose tissue (Fig. 1H and Supplementary Fig. S1A).

Considering that LPS-induced septic shock results from excessive stimulation of host immune cells, particularly monocytes and macrophages [22], primary peritoneal macrophages were harvested and treated with 1 μg/mL of LPS for 6 h to investigate the mechanism involved in this protective effect of CerS6 KO mice against LPS-induced sepsis. Similar to the lung data (Fig. 1H), ER stress, iNOS, NF-κB, MAP kinase, and inflammasome signaling pathways were activated by LPS in WT macrophages with concomitant production of IL-1β. However, LPS-induced activation of these cascades was strikingly normalized in CD36 KO macrophages (Fig. 2A). CerS6 expression elevated by LPS treatment was also reduced in CD36 KO macrophages. Consistently, the lack of CD36 in primary macrophages led to the alleviation of pro-inflammatory cytokine production as well as nitrite formation induced by LPS (Fig. 2B–E). In light of the marked reduction of CerS6 expression in primary peritoneal macrophages of CD36 KO mice (Fig. 2A), ceramide acyl chain length was measured in macrophages harvested from WT and CD36 KO mice. LPS administration significantly increased C16- and C18-ceramide levels in WT macrophages (Fig. 2F). In accordance with

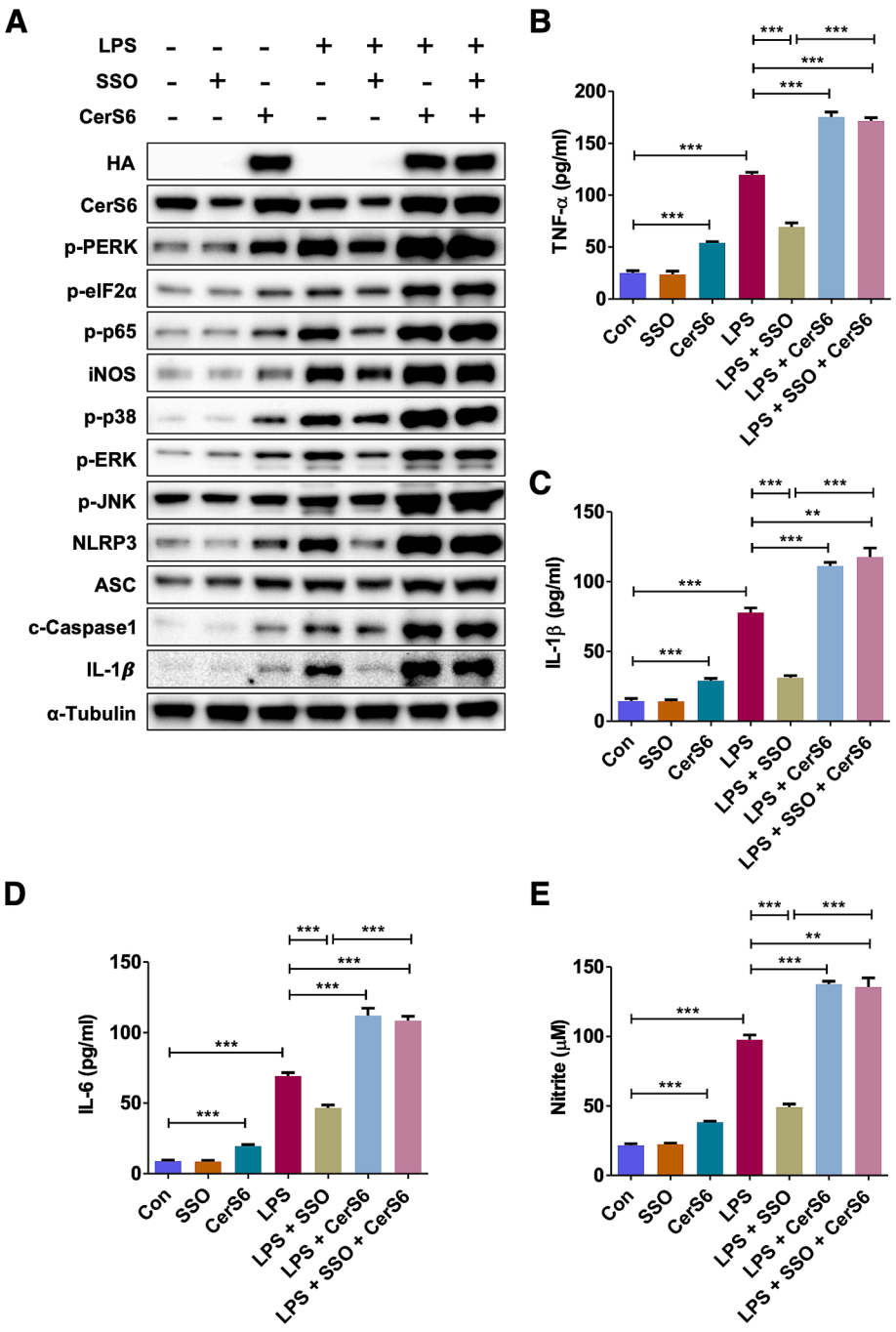


**Fig. 5. CerS6 overexpression restores LPS-induced inflammatory responses hampered by CD36 inhibition.** (**A**) WB of RAW264.7 cells with combinational treatment of LPS (50 ng/mL, 18 h) and SSO (100 μM, 30 h) under CerS6 overexpression. Levels of (**B**) TNF-α, (**C**) IL-1β, (**D**) IL-6, and (**E**) nitrite were measured in RAW264.7 cell culture medium using ELISA kits and Griess reagent ($n = 5$). The values are expressed as means ± S.E.M. $^{**}p < 0.01$, $^{***}p < 0.001$.

the reduction in CerS6 expression (Fig. 2A), C16-ceramide levels of CD36 KO macrophages were significantly reduced compared to WT macrophages in LPS-treated groups (Fig. 2F). In contrast to changes in CerS protein levels, the relative mRNA expression of six *CerS* was not significantly altered in CD36 KO macrophages compared to their WT counterparts (Supplementary Fig. S1B).

### 3.2. LPS increases the expression of CerS1 and CerS6

To investigate how CD36 deficiency in macrophages leads to CerS6 downregulation and protection against LPS-induced inflammation, we used a murine macrophage cell line, RAW264.7, to further explore the mechanism. Similar to primary peritoneal macrophages (Fig. 2B–E), LPS treatment in RAW264.7 cells significantly enhanced inflammation in a dose-dependent manner, as noted by the secretion of TNF-α, IL-1β, and IL-6 (Fig. 3A–C). Nitrite formed by NOS, mediating conversion of L-arginine to L-citrulline, was also increased by LPS in RAW264.7 cells (Fig. 3D). Having established that C16- and C18-ceramide levels were elevated by LPS injection in WT macrophages (Fig. 2F), we then examined whether LPS treatment alters ceramide acyl chain length and CerS expression in RAW264.7 cells. Similar to primary macrophage data (Fig. 2F), C16- and C18-ceramide levels were dose-dependently elevated in LPS-treated RAW264.7 cells (Fig. 3E). In addition, LPS (1 μg/mL) treatment also increased CerS1 and CerS6 mRNA (Fig. 3F) and protein

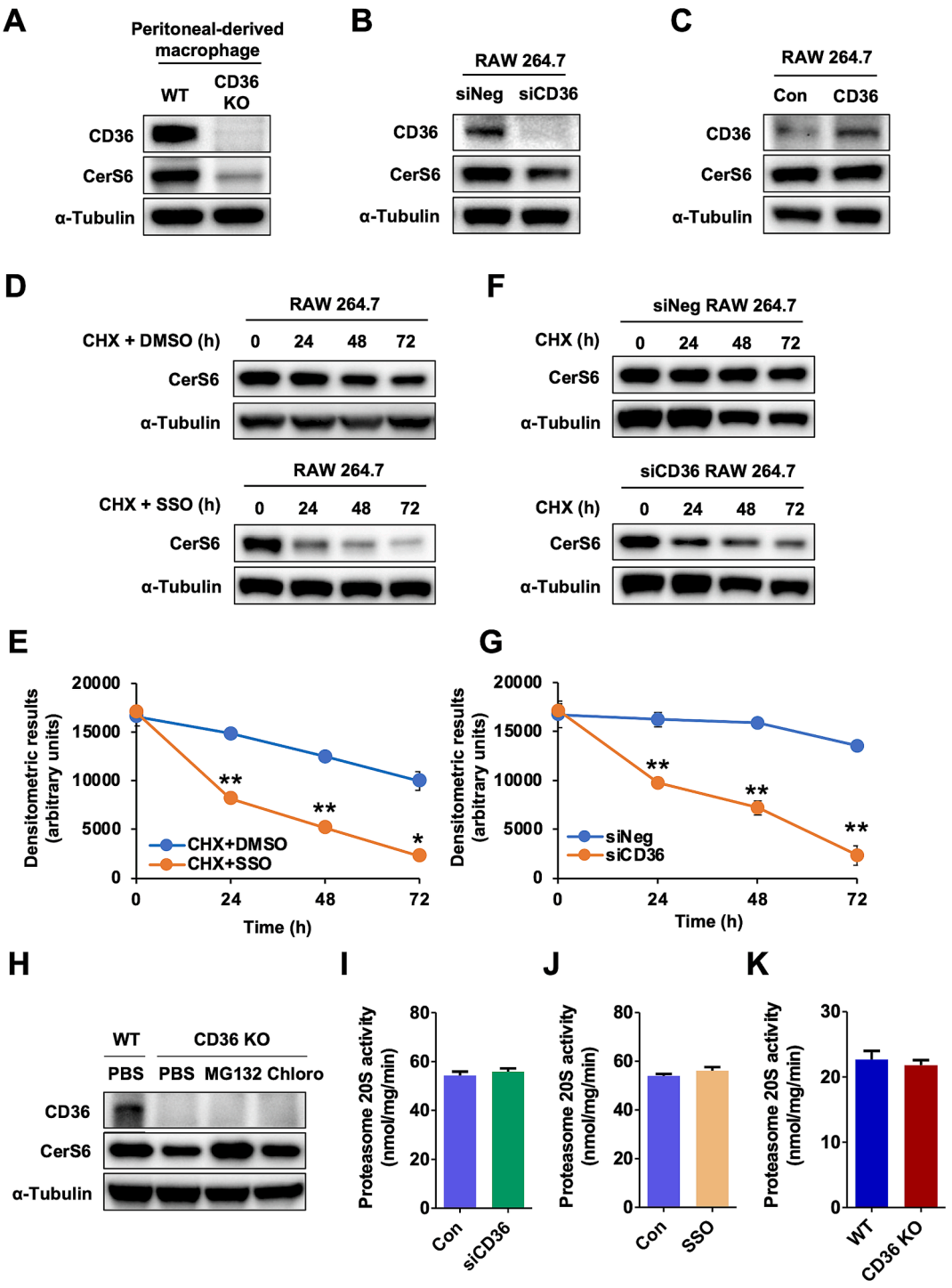


**Fig. 6. CD36 inhibition promotes proteasomal degradation of CerS6.** (**A**) Representative WB of peritoneal-derived macrophages of WT and CD36 KO mice. WB of RAW264.7 cells transfected with (**B**) siRNA for CD36 or (**C**) pcDNA6-CD36. (**D**) WB of a CHX chase in RAW264.7 cells treated with a CD36 inhibitor, SSO (100 μg/mL), and (**E**) its quantification using ImageJ (NIH, Bethesda, MD). (**F**) WB of a CHX chase in RAW264.7 cells transfected with siRNA for CD36 and (**G**) its quantification using ImageJ. (**H**) WB of peritoneal-derived macrophages of WT and CD36 KO mice treated with MG132 (a proteasome inhibitor, 1 μM) or chloroquine (a lysosome inhibitor, 1 μM) for 24 h. Proteasome 20S activity of RAW264.7 cells (**I**) transfected with siRNA for CD36 or (**J**) treated with a CD36 inhibitor, SSO (100 μg/mL, 24 h). (**K**) Proteasome 20S activity of peritoneal-derived macrophages derived from WT and CD36 KO mice. The values are expressed as means ± S.E.M. $^{**}p < 0.01$, $^{***}p < 0.001$.

levels (Fig. 3G). LPS stimulation at 50 ng/mL in TLR4-overexpressed RAW264.7 cells, but not in non-transfected RAW264.7 cells, enhanced CerS1 and CerS6 protein expressions, followed by amplification of inflammatory signaling cascades (Supplementary Fig. S2A) and production of cytokines and nitrite (Supplementary Fig. S2B–E). These data implicate that TLR4 stimulation above a certain threshold may be required to elevate CerS1 or CerS6 expression by LPS.

### 3.3. CD36 inhibition promotes CerS6 protein degradation linked to LPS-induced inflammatory response

Given that LPS-induced inflammatory response was markedly

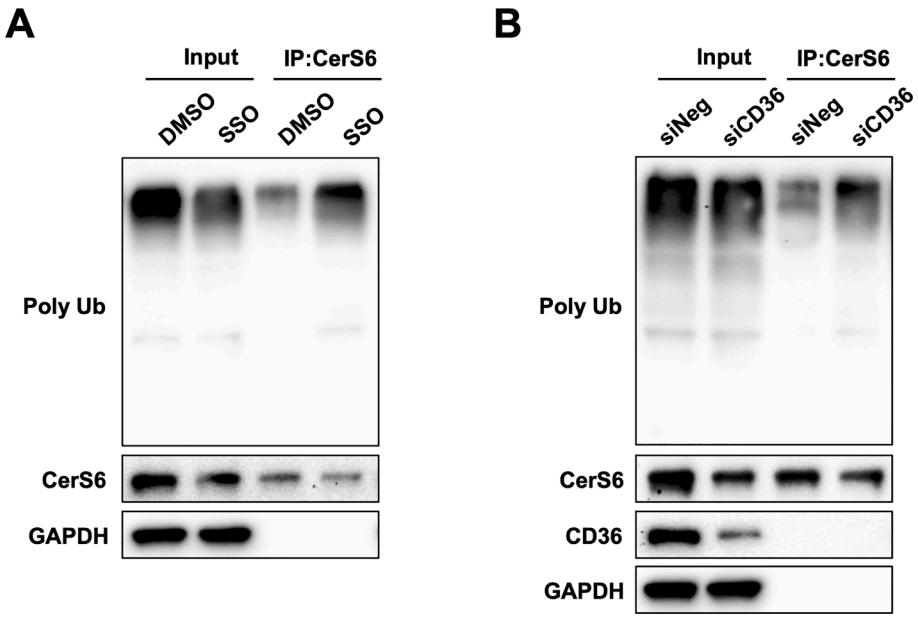


**Fig. 7. CD36 inhibition enhances CerS6 ubiquitination.** Representative WB of indicated antibodies after immunoprecipitation using CerS6 antibody in RAW264.7 cells upon (**A**) treatment with SSO (100 μg/mL, 24 h) or (**B**) transfection with siRNA for CD36.

diminished in CD36 KO mice, in which CerS6 protein expression was also reduced (Fig. 1H, Fig. 2A, and Supplementary Fig. S1A), we next investigated whether CD36 is directly involved in the modulation of CerS6 and LPS-induced inflammation. SSO irreversibly binds and inhibits CD36 [23]. In accordance with CerS6 reduction in CD36 KO mice (Fig. 1H, Fig. 2A, and Supplementary Fig. S1A), either CD36 inhibition using SSO or CD36 knockdown using RNA interference markedly reduced CerS6 protein levels as well as inflammatory signaling cascades, such as ER stress, iNOS, MAP kinase, and inflammasome (Fig. 4A and Supplementary Fig. S3A). Consistently, CD36 inhibition with SSO treatment or CD36 knockdown partially normalized LPS-induced cytokine and nitrite generation (Fig. 4B–E and Supplementary Fig. S3B–E).

To further elucidate whether CD36 inhibition exerts anti-inflammatory effect via CerS6 reduction, we overexpressed CerS6 under CD36 inhibition. CerS6 overexpression restored CerS6 protein levels reduced by CD36 inhibition, reactivating inflammatory signaling cascades including ER stress, iNOS, MAP kinase, and inflammasome, which were inhibited by CD36 inhibition (Fig. 5A). LPS-induced cytokine and nitrite generation were also reinduced by CerS6 overexpression under CD36 inhibition (Fig. 5B–E), confirming that CD36 inhibition mitigates the LPS-induced inflammatory response via reduced CerS6 expression.

We then explored whether CD36 and CerS6 inter-regulate each other. Decreased CD36 levels either in CD36 KO macrophages or in siCD36-transfected RAW264.7 cells caused a reduction in CerS6 protein levels (Fig. 6A and B). However, CD36 overexpression in RAW264.7 cells did not alter CerS6 expression (Fig. 6C), and neither CerS6 overexpression nor knockdown regulated CD36 protein levels (Supplementary Fig. S4A and B). To examine whether CD36 inhibition alters CerS6 protein degradation, a CHX chase assay was performed with SSO or siCD36. CD36 inhibition using either SSO (Fig. 6D and E) or CD36 knockdown (Fig. 6F and G) accelerated CerS6 degradation, which was recovered by proteasomal inhibition but not by lysosomal inhibition (Fig. 6H). However, 20S proteasome activity was not directly altered in both CD36-inhibited RAW264.7 cells and CD36 KO macrophages (Fig. 6I–K).

### 3.4. CD36 inhibition induces CerS6 ubiquitination

A variety of proteins are degraded via the ubiquitin−proteasome system, and ubiquitination marks proteins for proteasomal degradation [24]. Given that CD36 inhibition increased CerS6 protein degradation, causing markedly reduced CerS6 levels, which was hampered by blocking the proteasome (Fig. 6D–H), ubiquitination of CerS6 was further examined under CD36 inhibition. Not only SSO treatment but also CD36 knockdown enhanced CerS6 ubiquitination (Fig. 7A and B). However, total cellular ubiquitination was not altered by CD36 inhibition (Fig. 7A and B). These data collectively indicate that CD36 inhibition escalates CerS6 protein degradation via specifically targeting the ubiquitination of CerS6.

### 3.5. CerS6 partially mediates LPS-induced inflammation

To examine the effect of CerS1 and CerS6 in LPS-induced inflammation, either CerS1 or CerS6 was then transfected in RAW264.7 cells. CerS1 or CerS6 overexpression was confirmed by WB (Fig. 8A and Supplementary Fig. S5A). CerS1 overexpression did not alter inflammatory signaling cascades, including NF-κB, MAP kinase, and inflammasome pathways in RAW264.7 cells, irrespective of LPS treatment (Supplementary Fig. S5A). Consistently, the production of cytokines and nitrite was not changed by CerS1 overexpression (Supplementary Fig. S5B–E).

CerS6 overexpression elevated C16-ceramide levels, as measured using LC-ESI-MS/MS (Fig. 8B). In accordance with the relevant literature [12], CerS6 overexpression both induced ER stress and further aggravated LPS-induced ER stress (Fig. 8C). In addition, CerS6 also propagated and amplified iNOS, NF-κB, MAP kinase, and inflammasome signaling cascades in LPS-treated RAW264.7 cells (Fig. 8A) with concomitant elevation of pro-inflammatory cytokine production (Fig. 8D–F). Increased iNOS expression by CerS6 overexpression (Fig. 8A) was also accompanied by elevated nitrite content (Fig. 8G).

Next, shCerS6 was transfected in RAW264.7 cells to examine whether CerS6 downregulation exhibits the opposite effect. Transfection of shCerS6 reduced CerS6 protein levels, and LPS-induced activation of signaling pathways, such as ER stress, MAP kinase, and inflammasome, was abrogated by CerS6 downregulation (Fig. 9A). CerS6 downregulation also significantly diminished LPS-induced pro-inflammatory cytokine production (TNF-α, IL-1β, and IL-6) and nitrite formation (Fig. 9B–E). These data indicate that CerS6 mediates the LPS-induced inflammatory response by modulating ER stress, MAP kinase, and

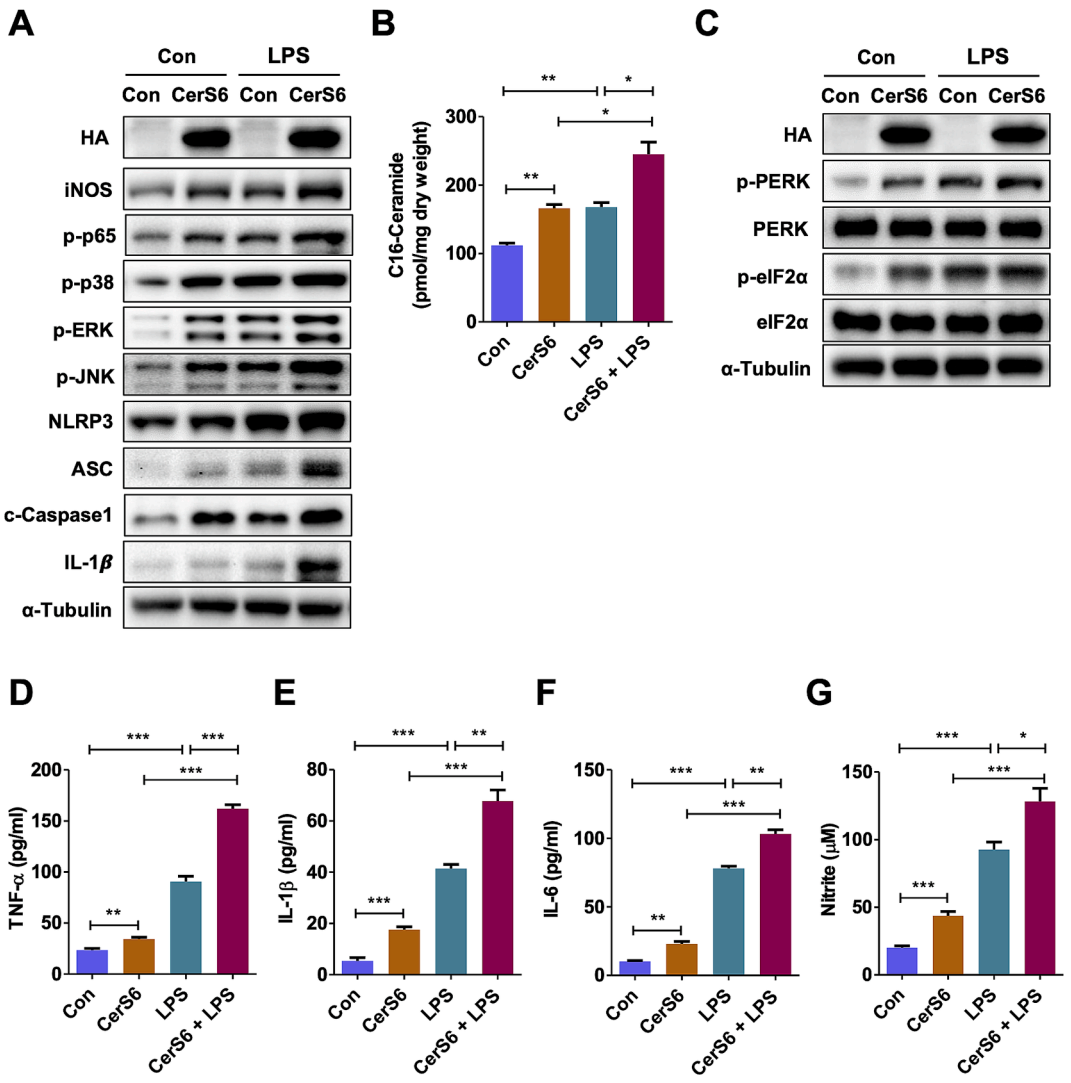


**Fig. 8. CerS6 overexpression augments LPS-induced inflammatory response.** (**A**) WB of RAW264.7 cells transfected with CerS6, followed by LPS (50 ng/mL) treatment for 18 h. (**B**) C16-ceramide levels were measured by LC-ESI-MS/MS ($n = 3$). (**C**) WB of CerS6-overexpressed RAW264.7 cells in the presence or absence of LPS stimulation (50 ng/mL, 18 h). Levels of (**D**) TNF-α, (**E**) IL-1β, (**F**) IL-6, and (**G**) nitrite were measured in RAW264.7 cell culture medium using ELISA kits and Griess reagent ($n = 5$). The values are expressed as means ± S.E.M. $^{*}p < 0.05$, $^{**}p < 0.01$, $^{***}p < 0.001$.

inflammasome cascades.

### 3.6. ER stress is the upstream signaling cascade for MAP kinase and inflammasome pathways

Considering that CerS6 not only induces ER stress but also aggravates LPS-induced ER stress (Fig. 8C), we then investigated the role of ER stress in LPS-induced inflammatory response. Thapsigargin induces ER stress via inhibiting sarco/ER $Ca^{2+}$-ATPase activity, causing an imbalance in $Ca^{2+}$ homeostasis [25]. To induce ER stress, RAW264.7 cells were treated with 300 nM thapsigargin combined with 50 ng/mL of LPS. Thapsigargin induced ER stress similar to LPS treatment in RAW264.7 cells, and thapsigargin addition in LPS-treated RAW264.7 cells amplified ER stress, as shown by PERK and eIF2α phosphorylation (Fig. 10A). Without LPS, thapsigargin alone activated NF-κB, MAP kinase, and inflammasome pathways, similar to LPS treatment (Fig. 10A). In addition, thapsigargin and LPS co-treatment markedly amplified signaling cascades, including NF-κB, MAP kinase, and inflammasome (Fig. 10A).

Next, we co-treated TUDCA or 4-PBA with LPS to explore whether ER stress inhibition can alleviate LPS-induced signaling activation. TUDCA hampers the dissociation between glucose-regulated protein 78 (GRP78) and PERK [26], and 4-PBA acts as a chemical chaperone, inhibiting ER stress [27]. Co-treatment of these chemical compounds with LPS in RAW264.7 cells markedly inhibited LPS-induced activation of ER stress accompanied by reduction of NF-κB, MAP kinase, and inflammasome signaling (Fig. 10B). Finally, the LPS-induced generation of cytokines and nitrite was examined to confirm the effect of ER stress modulation on the LPS-induced inflammatory response. In accordance with signaling cascades (Fig. 10B), LPS-induced cytokine and nitrite production was partially diminished by TUDCA or 4-PBA (Fig. 10C–F). These data implicate that ER stress modulates downstream signaling pathways, such as NF-κB, MAP kinase, and inflammasome, and regulates the LPS-induced inflammatory response.

### 3.7. CerS6 modulates LPS-induced inflammatory response via ER stress

Finally, we explored whether CerS6-mediated amplification of LPS-induced inflammation is exerted via ER stress. Both ER stress inhibition using 4-PBA as well as CerS inhibition using fumonisin B1 [28] reduced CerS6-mediated activation of NF-κB, MAP kinase, and inflammasome signaling cascades (Fig. 11A). Furthermore, CerS6-mediated amplification of LPS-induced signaling activation was also markedly abrogated by either 4-PBA or fumonisin B1 (Fig. 11A). In addition, LPS-induced formation of cytokines, such as TNF-α, IL-1β, and IL-6, was also

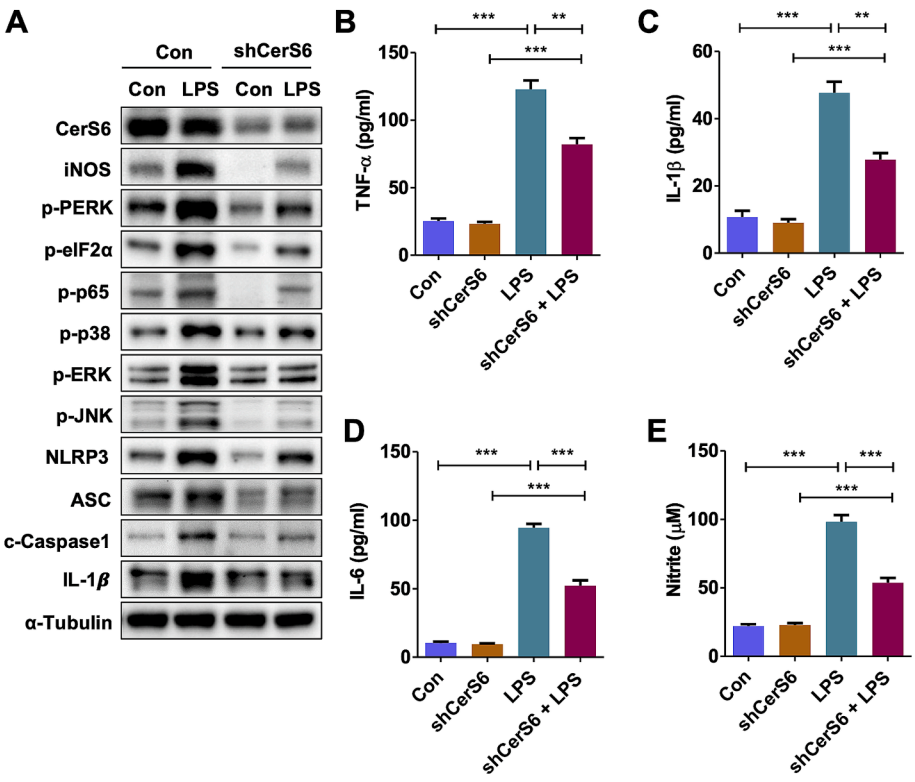


**Fig. 9. CerS6 downregulation reduces LPS-induced inflammatory response.** (**A**) WB of RAW264.7 cells sequentially treated with shRNA against CerS6 (48 h) and LPS (50 ng/mL, 18 h). Levels of (**B**) TNF-α, (**C**) IL-1β, (**D**) IL-6, and (**E**) nitrite were measured in RAW264.7 cell culture medium using ELISA kits and Griess reagent ($n = 5$). The values are expressed as means ± S.E.M. $^{**}p < 0.01$, $^{***}p < 0.001$.

augmented by CerS6, and 4-PBA or fumonisin B1 treatment partially normalized the aggravating effect of CerS6 on LPS-induced cytokine formation (Fig. 11B–D). These results indicate that CerS6-derived C16-ceramide augments LPS-induced inflammation via ER stress.

## 4. Discussion

Macrophages have a central role in inflammation. In the present study, we examined the effects of ceramide acyl chain length on the LPS-induced inflammatory response in RAW264.7 cells. LPS increased both the mRNA and protein levels of CerS6, leading to the elevation of C16-ceramide. CerS6-derived C16-ceramide augmented the LPS-induced inflammatory response via propagating ER stress, which further activated downstream signaling pathways, such as NF-κB and inflammasome.

LPS has been previously known to induce pro-inflammatory cytokines through MAP kinase and NF-κB pathways [29,30], and the present study suggests CerS6-activated ER stress as an upstream regulator of these pathways. Inhibition of CerS by fumonisin B1 also abrogated the amplifying effect of CerS6 on LPS-induced inflammation, demonstrating that CerS6-derived ceramide generation plays a critical role in LPS-induced inflammation. Regulation of ER stress by CerS and its derivatives, ceramide species, has been previously reported [12,31–33]. Obesity-associated elevation of CerS6-derived C16-ceramide promoted ER/mitochondrial stress in hypothalamic neurons and had a pivotal role in the deregulation of food intake and glucose metabolism [32]. We have previously reported the detrimental effect of CerS6 in hepatic ER stress, which contributes to lipogenesis and fatty liver progression [12]. On the contrary, CerS2 and C24-ceramide inhibited ER stress and sterol regulatory element-binding protein 1 (SREBP1) cleavage, resulting in protection against fatty liver disease progression [12]. A recent study also showed that exogenous C2-ceramide caused ER stress, as demonstrated by increased levels of phosphorylated eIF2α and spliced X-box-binding protein-1 (XBP1) via inducing $[Ca^{2+}]_{ER}$ depletion [33]. The activation of activating transcription factor 6 (ATF-6) via perturbation of cellular $Ca^{2+}$ has also been suggested as a mechanism for the induction of ER stress by CerS6 and its derivative, C16-ceramide [34]. The present study recapitulated the role of CerS6 in ER stress, which modulated LPS-induced inflammatory response and sepsis.

The present study also revealed the regulation of CerS6 by CD36. Reduced CerS6 protein levels were observed not only in peritoneal macrophages but also in the lung, liver, skeletal muscle, and adipose tissues of CD36 KO mice. However, *CerS6* mRNA levels in CD36 KO mice were not altered in CD36 KO macrophages. Furthermore, MG132 treatment restored CerS6 protein levels in CD36 KO macrophages, suggesting the proteasomal degradation of CerS6. Accordingly, CD36 inhibition markedly elevated CerS6 ubiquitination targeting for proteasomal degradation. The regulation of ubiquitination of several proteins by CD36 has been previously reported [35,36]. For example, in acute kidney injury, CD36 binds to ferroptosis suppressor protein 1 (FSP1) and accelerates its degradation via inducing ubiquitination [36]. Similarly, CD36-Glypican 4 (GPC4) interaction in colorectal cancer promotes GPC4 ubiquitination, leading to its proteasomal degradation [35]. However, in the present study, CD36 – CerS6 interaction was not observed in an immunoprecipitation assay, and only CD36 inhibition, but not CD36 overexpression, modulated CerS6 protein levels. Therefore, the regulation of CerS6 protein stability by CD36 might not be the primary consequence. For example, CD36 inhibition would escalate CerS6 ubiquitination, possibly via regulating enzymes involved in ubiquitination or deubiquitination targeting CerS6. Despite the unsolved mechanisms, the reduction of CerS6 protein levels by CD36 blockage was consistent and could be efficiently applied to control endotoxin-induced inflammation.

SLs are one of the major components of the lipid raft in which CD36 is located [37], and alteration of ceramide acyl chain length by CerS modulation can affect lipid raft properties, which ultimately impacts the function of proteins located in the lipid raft [38,39]. We previously

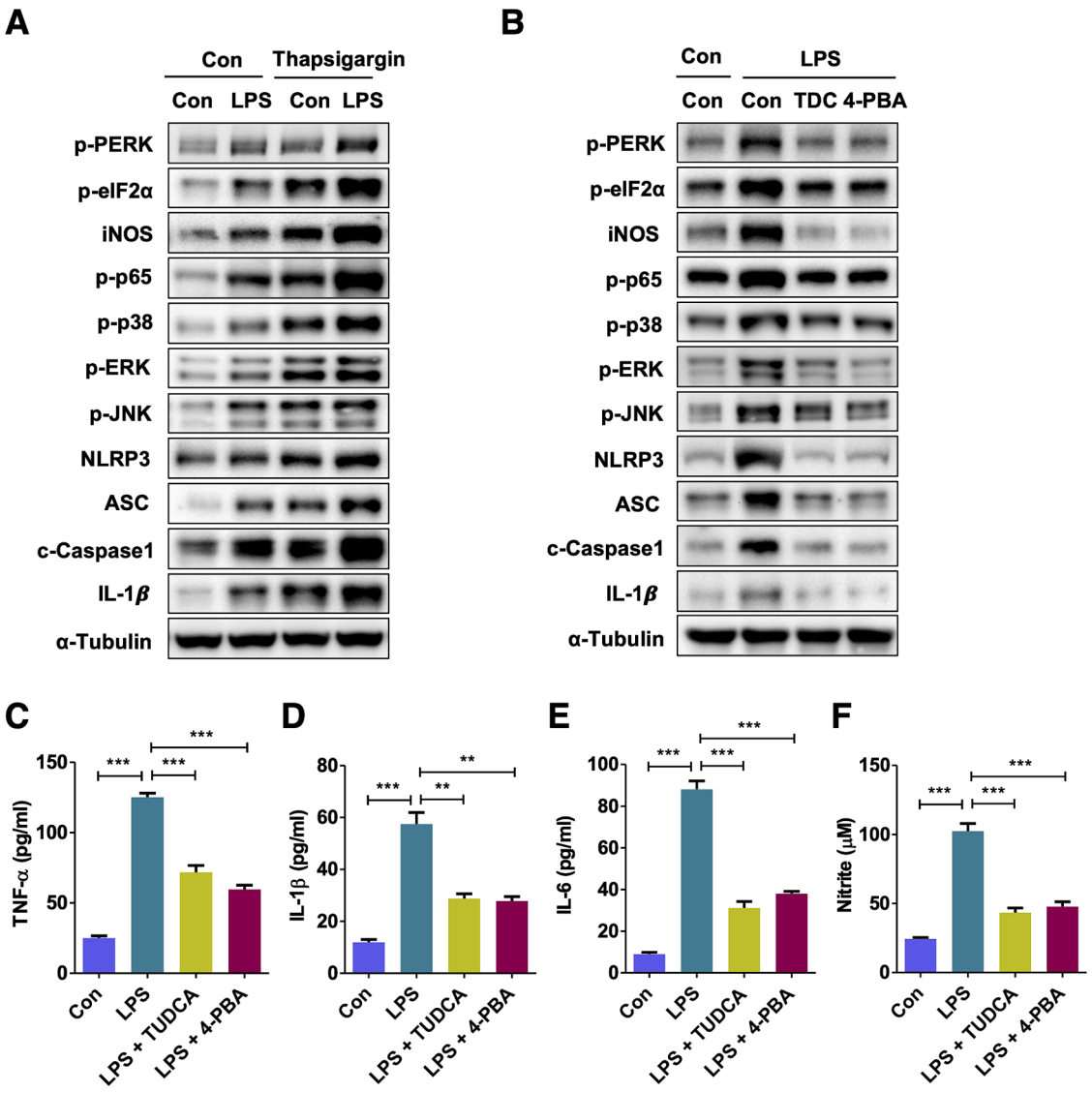


**Fig. 10. ER stress regulates NF-κB, MAP kinase, and inflammasome signaling cascades during LPS-induced inflammatory response.** (**A**) WB of RAW264.7 cells with combinational treatment of LPS (50 ng/mL, 18 h) and thapsigargin (300 nM, 18 h). (**B**) WB of RAW264.7 cells treated with LPS (50 ng/mL, 18 h) in the presence or absence of TUDCA (500 μM, 30 h) or 4-PBA (5 mM, 30 h). Levels of (**C**) TNF-α, (**D**) IL-1β, (**E**) IL-6, and (**F**) nitrite were measured in RAW264.7 cell culture medium using ELISA kits and Griess reagent ($n = 5$). The values are expressed as means ± S.E.M. $^{**}p < 0.01$, $^{***}p < 0.001$.

reported that ablation of CerS2, which causes deficiency of C22−C24-ceramides, led to lipid raft alteration [38] and mislocalization of CD36 [40]. Another group also showed that either the addition of synthetic short-chain ceramides or activation of sphingomyelinase to generate physiological long-chain ceramides resulted in significant reductions in CD36 expression, not by inhibition of mRNA expression but by blockade of CD36 trafficking to the membrane in monocytes/macrophages [41]. These studies suggest that CD36 can be regulated by altered ceramide composition. Conversely, the current study demonstrated that CD36 alters ceramide acyl chain length by regulating CerS6 protein stability and degradation. Therefore, CerS-derived ceramide and CD36 may interact bidirectionally.

LPS treatment of RAW264.7 cells elevated C16- and C18-ceramides dose-dependently. Increased C16- and C18-ceramides upon LPS treatment at 1 μg/mL coincided with the elevation of mRNA and protein expressions of CerS1 and CerS6. However, LPS treatment at 50 ng/mL still increased C16- and C18-ceramides without altering either CerS1 or CerS6 expressions. Although regulation of CerS activity by 50 ng/mL of LPS can be possible, the exact mechanism of this phenomenon remains to be elucidated. In contrast to non-transfected cells, the 50 ng/mL LPS treatment of TLR4-overexpressed RAW264.7 cells elevated CerS1 and CerS6 protein expressions similar to 1 μg/mL of LPS, suggesting that TLR4 stimulation above a certain threshold may be required to enhance the expression of CerS1 and CerS6.

Despite CerS5 and CerS6 generating C16-ceramide in common, the impact of CerS5 or CerS6 on inflammatory signaling pathways was completely different in RAW264.7 cells (Supplementary Fig. S6). Only CerS6, but not CerS5, activated NF-κB, MAP kinase, and inflammasome signaling pathways (Supplementary Fig. S6A) with concomitant increase of cytokine and nitrite formation (Supplementary Fig. S6B–E). The distinct effects of these two proteins on a variety of intracellular events have already been reported [12]. Considering that ER stress, which is the upstream regulator of NF-κB, MAP kinase, and inflammasome signaling pathways during LPS stimulation, has not been affected by CerS5 in palmitate-treated Hep3B cells [12], CerS5 may not alter these inflammatory signaling cascades due to no impact on ER stress. Similarly, CerS1 did not affect the LPS-induced inflammatory response. In addition, given that CerS1 expression is extremely low in RAW264.7 cells (Supplementary Fig. S7), CerS1 would play only a minor role in the LPS-induced inflammatory process in macrophages. The present results

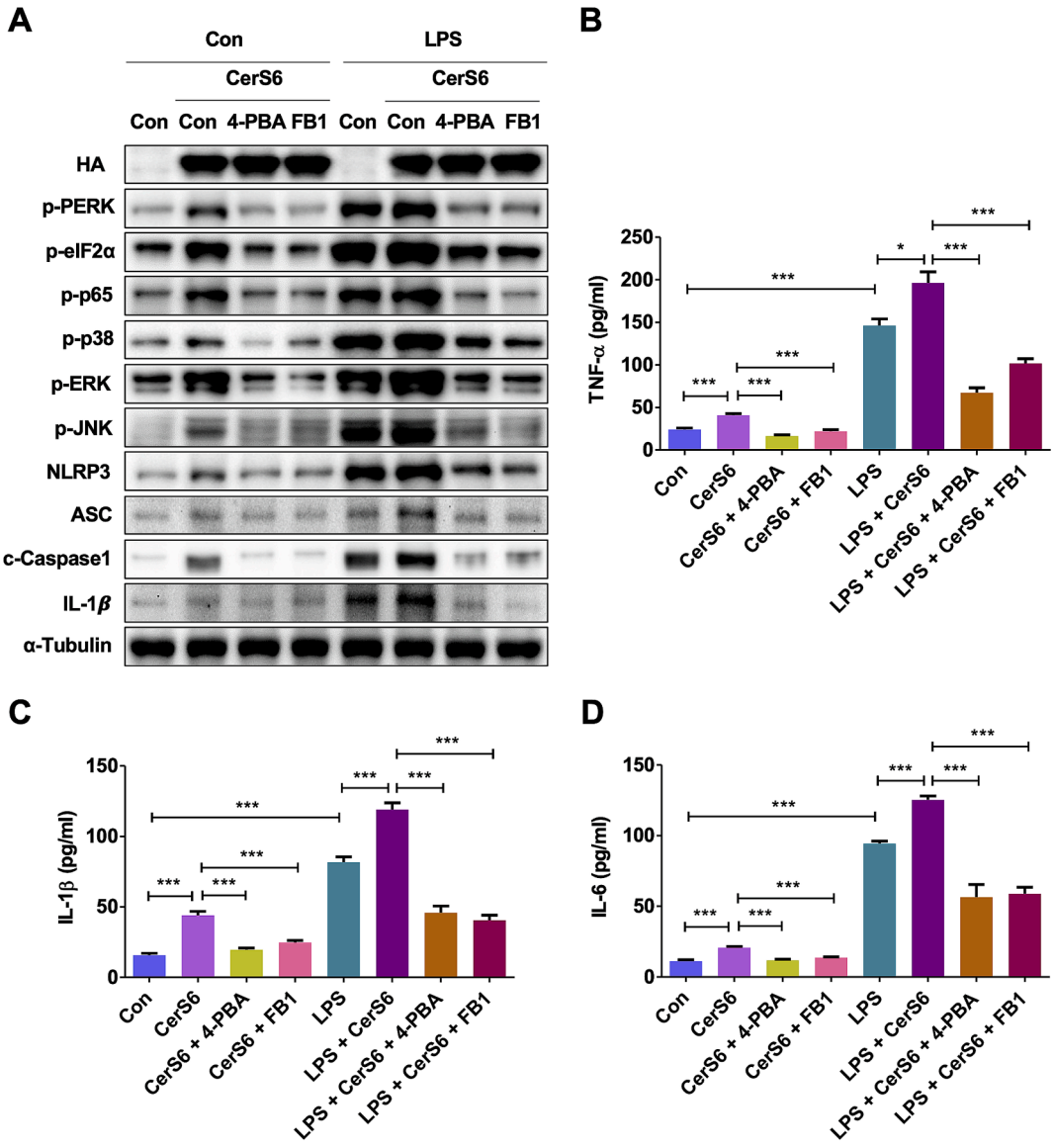


**Fig. 11. CerS6-derived C16-ceramide amplifies LPS-induced inflammatory response via ER stress.** (**A**) WB of CerS6-overexpressed RAW264.7 cells with combinational treatment of LPS (50 ng/mL, 48 h), 4-PBA (5 mM, 30 h), and FB1 (1 μM, 30 h). Levels of (**B**) TNF-α, (**C**) IL-1β, and (**D**) IL-6 were measured in RAW264.7 cell culture medium using ELISA kits and Griess reagent ($n = 5$). The values are expressed as means ± S.E.M. $^{*}p < 0.05$, $^{***}p < 0.001$.

are in accordance with the relevant literature reporting that only CerS6, but not other CerS isoforms, increases TNF-α secretion in Hep3B cells [30].

## 5. Conclusion

CerS attaches a fatty acid to a long-chain base via an amide bond, and CD36 functions as a fatty acid transporter. Considering critical roles of both proteins in lipid metabolism, mutual influence would have a functional role in biology. The current study provides evidence that CD36 functions as an upstream regulator of CerS6, regulating CerS6 protein stability and degradation, by which CD36 eventually plays a pivotal role in LPS-induced septic response. Mechanistically, CerS6-derived C16-ceramide amplifies LPS-induced inflammatory signaling cascades by modulating ER stress in macrophages, and CD36-induced CerS6 reduction could mitigate endotoxin-induced inflammatory response. Collectively, the current study suggests that targeting CD36 or CerS6 would be an efficacious strategy for managing endotoxin-induced septic shock and inflammation.

## Funding Sources

Funding: This work was supported by National Research Foundation (NRF) of Korea grants funded by the Korean government, the Ministry of Science and ICT [NRF-2021R1A5A2030333 to W-J.P., B-C.O., and Y.J.; NRF-2022R1A2C1006737 to J-W.P.; and NRF-2022R1I1A1A0106408112 to MH.K.].

## CRediT authorship contribution statement

**Min Hee Kim:** Validation, Investigation, Funding acquisition, Formal analysis, Data curation, Conceptualization. **Hyomin Lim:** Validation, Methodology, Investigation, Formal analysis. **Ok-Hee Kim:** Resources, Methodology, Data curation. **Byung-Chul Oh:** Resources, Conceptualization. **YunJae Jung:** Validation, Methodology, Conceptualization. **Kyung-Ha Ryu:** Resources, Conceptualization. **Joo-Won Park:** Writing – review & editing, Funding acquisition, Data curation, Conceptualization. **Woo-Jae Park:** Writing – review & editing, Writing – original draft, Supervision, Investigation, Funding acquisition, Conceptualization.

## Declaration of Competing Interest

The authors declare that they have no known competing financial interests or personal relationships that could have appeared to influence the work reported in this paper.

## Acknowledgments

Plasmids (pcDNA3.1-CerS1-HA, pcDNA3.1-CerS5-HA, pcDNA3.1-CerS6-HA, and pSUPER-shCerS6) were kindly provided by Professor Anthony H. Futerman (Weizmann Institute of Science, Rehovot, Israel).

## Appendix A. Supplementary data

Supplementary data to this article can be found online at https://doi.org/10.1016/j.intimp.2024.113441.

## Data availability

No data was used for the research described in the article.

## References

[1] M. Singer, C.S. Deutschman, C.W. Seymour, M. Shankar-Hari, D. Annane, M. Bauer, R. Bellomo, G.R. Bernard, J.-D. Chiche, C.M. Coopersmith, R.S. Hotchkiss, M. M. Levy, J.C. Marshall, G.S. Martin, S.M. Opal, G.D. Rubenfeld, T. van der Poll, J.-L. Vincent, D.C. Angus, The third international consensus definitions for sepsis and septic shock (Sepsis-3), JAMA 315 (8) (2016) 801–810, https://doi.org/10.1001/jama.2016.0287.

[2] R. Meilik, H. Ben-Assayag, A. Meilik, S. Berliner, D. Zeltser, I. Shapira, O. Rogowski, I. Goldiner, S. Shenhar-Tsarfaty, A. Wasserman, Sepsis related mortality associated with an inflammatory burst in patients admitting to the Department of Internal Medicine with apparently normal C-reactive protein concentration, J. Clin. Med. 11 (11) (2022) 3151, https://doi.org/10.3390/jcm11113151.

[3] C. Nedeva, J. Menassa, H. Puthalakath, Sepsis: inflammation is a necessary evil, Front Cell Dev. Biol. 7 (2019) 108, https://doi.org/10.3389/fcell.2019.00108.

[4] M. Wang, J. Feng, D. Zhou, J. Wang, Bacterial lipopolysaccharide-induced endothelial activation and dysfunction: a new predictive and therapeutic paradigm for sepsis, Eur. J. Med. Res. 28 (1) (2023) 339, https://doi.org/10.1186/s40001-023-01301-5.

[5] J.-M. Cavaillon, M. Adib-Conquy, Monocytes/macrophages and sepsis, Crit. Care. Med. 33 (12 Suppl) (2005) S506–S509, https://doi.org/10.1097/01.ccm.0000185502.21012.37.

[6] G.F. Nixon, Sphingolipids in inflammation: pathological implications and potential therapeutic targets, Br. J. Pharmacol. 158 (4) (2009) 982–993, https://doi.org/10.1111/j.1476-5381.2009.00281.x.

[7] W.-J. Park, J.-W. Park, The effect of altered sphingolipid acyl chain length on various disease models, Biol. Chem. 396 (6–7) (2015) 693–705, https://doi.org/10.1515/hsz-2014-0310.

[8] J.-W. Park, W.-J. Park, A.H. Futerman, Ceramide synthases as potential targets for therapeutic intervention in human diseases, Biochim. Biophys. Acta 1841 (5) (2014) 671–681, https://doi.org/10.1016/j.bbalip.2013.08.019.

[9] W.-J. Park, J.-W. Park, The role of sphingolipids in endoplasmic reticulum stress, FEBS Lett. 594 (22) (2020) 3632–3651, https://doi.org/10.1002/1873-3468.13863.

[10] M. Eberle, P. Ebel, C.A. Mayer, J. Barthelmes, N. Tafferner, N. Ferreiros, T. Ulshöfer, M. Henke, C. Foerch, A.M. de Bazo, S. Grösch, G. Geisslinger, K. Willecke, S. Schiffmann, Exacerbation of experimental autoimmune encephalomyelitis in ceramide synthase 6 knockout mice is associated with enhanced activation/migration of neutrophils, Immunol. Cell Biol. 93 (9) (2015) 825–836, https://doi.org/10.1038/icb.2015.47.

[11] J. Barthelmes, A.M. de Bazo, Y. Pewzner-Jung, K. Schmitz, C.A. Mayer, C. Foerch, M. Eberle, N. Tafferner, N. Ferreirós, M. Henke, G. Geisslinger, A.H. Futerman, S. Grösch, S. Schiffmann, Lack of ceramide synthase 2 suppresses the development of experimental autoimmune encephalomyelitis by impairing the migratory capacity of neutrophils, Brain Behav. Immun. 46 (2015) 280–292, https://doi.org/10.1016/j.bbi.2015.02.010.

[12] Y.-R. Kim, E.-J. Lee, K.-O. Shin, M.H. Kim, Y. Pewzner-Jung, Y.-M. Lee, J.-W. Park, A.H. Futerman, W.-J. Park, Hepatic triglyceride accumulation via endoplasmic reticulum stress-induced SREBP-1 activation is regulated by ceramide synthases, Exp. Mol. Med. 51 (11) (2019) 1–16, https://doi.org/10.1038/s12276-019-0340-1.

[13] T. Sassa, S. Suto, Y. Okayasu, A. Kihara, A shift in sphingolipid composition from C24 to C16 increases susceptibility to apoptosis in HeLa cells, Biochim. Biophys. Acta 1821 (7) (2012) 1031–1037, https://doi.org/10.1016/j.bbalip.2012.04.008.

[14] M.M. Rogero, P.C. Calder, Obesity, inflammation, Toll-like receptor 4 and fatty acids, Nutrients 10 (4) (2018) 432, https://doi.org/10.3390/nu10040432.

[15] Y. Chen, J. Zhang, W. Cui, R.L. Silverstein, CD36, a signaling receptor and fatty acid transporter that regulates immune cell metabolism and fate, J. Exp. Med. 219 (6) (2022) e20211314.

[16] D. Cao, J. Luo, D. Chen, H. Xu, H. Shi, X. Jing, W. Zang, CD36 regulates lipopolysaccharide-induced signaling pathways and mediates the internalization of *Escherichia coli* in cooperation with TLR4 in goat mammary gland epithelial cells, Sci. Rep. 6 (2016) 23132, https://doi.org/10.1038/srep23132.

[17] A. Leelahavanichkul, A.V. Bocharov, R. Kurlander, I.N. Baranova, T. G. Vishnyakova, A.C. Souza, X. Hu, K. Doi, B. Vaisman, M. Amar, D. Sviridov, Z. Chen, A.T. Remaley, G. Csako, A.P. Patterson, P.S. Yuen, R.A. Star, T. L. Eggerman, Class B scavenger receptor types I and II and CD36 targeting improves sepsis survival and acute outcomes in mice, J. Immunol. 188 (6) (2012) 2749–2758, https://doi.org/10.4049/jimmunol.1003445.

[18] H.S. Baek, H.J. Min, V.S. Hong, T.K. Kwon, J.W. Park, J. Lee, S. Kim, Anti-inflammatory effects of the novel PIM kinase inhibitor KMU-470 in RAW 264.7 cells through the TLR4-NF-κB-NLRP3 pathway, Int J Mol Sci 21 (14) (2020) 5138, https://doi.org/10.3390/ijms21145138.

[19] K.M. Ajuwon, M.E. Spurlock, Palmitate activates the NF-κB transcription factor and induces IL-6 and TNFα expression in 3T3-L1 adipocytes, J. Nutr. 135 (8) (2005) 1841–1846, https://doi.org/10.1093/jn/135.8.1841.

[20] J. Yoon, H.-N. Um, J. Jang, Y.-A. Bae, W.-J. Park, H.J. Kim, M.-S. Yoon, I.Y. Chung, Y. Jung, Eosinophil activation by Toll-like receptor 4 ligands regulates macrophage polarization, Front Cell Dev. Biol. 7 (2019) 329, https://doi.org/10.3389/fcell.2019.00329.

[21] M.W. Pfaffl, A new mathematical model for relative quantification in real-time RT-PCR, Nucleic Acids Res. 29 (9) (2001) e45.

[22] L. Shapira, W.A. Soskolne, Y. Houri, V. Barak, A. Halabi, A. Stabholz, Protection against endotoxic shock and lipopolysaccharide-induced local inflammation by tetracycline: correlation with inhibition of cytokine secretion, Infect Immun. 64 (3) (1996) 825–828, https://doi.org/10.1128/iai.64.3.825-828.1996.

[23] O. Kuda, T.A. Pietka, Z. Demianova, E. Kudova, J. Cvacka, J. Kopecky, N. A. Abumrad, Sulfo-*N*-succinimidyl oleate (SSO) inhibits fatty acid uptake and signaling for intracellular calcium via binding CD36 lysine 164: SSO also inhibits oxidized low density lipoprotein uptake by macrophages, J. Biol. Chem. 288 (22) (2013) 15547–15555, https://doi.org/10.1074/jbc.m113.473298.

[24] H.-C. Tai, E.M. Schuman, Ubiquitin, the proteasome and protein degradation in neuronal function and dysfunction, Nat. Rev. Neurosci. 9 (11) (2008) 826–838, https://doi.org/10.1038/nrn2499.

[25] P. Sehgal, P. Szalai, C. Olesen, H.A. Praetorius, P. Nissen, S.B. Christensen, N. Engedal, J.V. Møller, Inhibition of the sarco/endoplasmic reticulum (ER) $Ca^{2+}$-ATPase by thapsigargin analogs induces cell death via ER $Ca^{2+}$ depletion and the unfolded protein response, J. Biol. Chem. 292 (48) (2017) 19656–19673, https://doi.org/10.1074/jbc.m117.796920.

[26] Y.M. Yoon, J.H. Lee, S.P. Yun, Y.S. Han, C.W. Yun, H.J. Lee, H. Noh, S.J. Lee, H. J. Han, S.H. Lee, Tauroursodeoxycholic acid reduces ER stress by regulating of Akt-dependent cellular prion protein, Sci. Rep. 6 (2016) 39838.

[27] H.-P. Pao, W.-I. Liao, S.-E. Tang, S.-Y. Wu, K.-L. Huang, S.-J. Chu, Suppression of endoplasmic reticulum stress by 4-PBA protects against hyperoxia-induced acute lung injury via up-regulating claudin-4 expression, Front Immunol 12 (2021) 674316, https://doi.org/10.3389/fimmu.2021.674316.

[28] N.C. Zitomer, T. Mitchell, K.A. Voss, G.S. Bondy, S.T. Pruett, E.C. Garnier-Amblard, L.S. Liebeskind, H. Park, E. Wang, M.C. Sullards, A.H. Merrill Jr., R.T. Riley, Ceramide synthase inhibition by fumonisin B1 causes accumulation of 1-deoxysphinganine: a novel category of bioactive 1-deoxysphingoid bases and 1-deoxydihydroceramides biosynthesized by mammalian cell lines and animals, J. Biol. Chem. 284 (8) (2009) 4786–4795, https://doi.org/10.1074/jbc.m808798200.

[29] D.W. Hommes, M.P. Peppelenbosch, S.J. van Deventer, Mitogen activated protein (MAP) kinase signal transduction pathways and novel anti-inflammatory targets, Gut. 52 (1) (2003) 144–151, https://doi.org/10.1136/gut.52.1.144.

[30] M.H. Kim, H.K. Ahn, E.-J. Lee, S.-J. Kim, Y.-R. Kim, J.-W. Park, W.-J. Park, Hepatic inflammatory cytokine production can be regulated by modulating sphingomyelinase and ceramide synthase 6, Int. J. Mol. Med. 39 (2) (2017) 453–462, https://doi.org/10.3892/ijmm.2016.2835.

[31] C.E. Senkal, S. Ponnusamy, J. Bielawski, Y.A. Hannun, B. Ogretmen, Antiapoptotic roles of ceramide-synthase-6-generated C16-ceramide via selective regulation of the ATF6/CHOP arm of ER-stress-response pathways, FASEB J. 24 (1) (2010) 296–308, https://doi.org/10.1096/fj.09-135087.

[32] P. Hammerschmidt, S.M. Steculorum, C.L. Bandet, A. Del Río-Martín, L. Steuernagel, V. Kohlhaas, M. Feldmann, L. Varela, A. Majcher, M. Quatorze Correia, R.F. Klar, C.A. Bauder, E. Kaya, M. Porniece, N. Biglari, A. Sieben, T. L. Horvath, T. Hornemann, S. Brodesser, J.C. Brüning, CerS6-dependent ceramide synthesis in hypothalamic neurons promotes ER/mitochondrial stress and impairs glucose homeostasis in obese mice, Nat. Commun. 14 (1) (2023) 7824, https://doi.org/10.1038/s41467-023-42595-7.

[33] Z. Liu, Y. Xia, B. Li, H. Xu, C. Wang, Y. Liu, Y. Li, C. Li, N. Gao, L. Li, Induction of ER stress-mediated apoptosis by ceramide via disruption of ER $Ca^{2+}$ homeostasis in human adenoid cystic carcinoma cells, Cell Biosci. 4 (2014) 71, https://doi.org/10.1186/2045-3701-4-71.

[34] C.E. Senkal, S. Ponnusamy, Y. Manevich, M. Meyers-Needham, S.A. Saddoughi, A. Mukhopadyay, P. Dent, J. Bielawski, B. Ogretmen, Alteration of ceramide synthase 6/$C_{16}$-ceramide induces activating transcription factor 6-mediated endoplasmic reticulum (ER) stress and apoptosis via perturbation of cellular $Ca^{2+}$ and ER/Golgi membrane network, J. Biol. Chem. 286 (49) (2011) 42446–42458, https://doi.org/10.1074/jbc.m111.287383.

[35] Y. Fang, Z.-Y. Shen, Y.-Z. Zhan, X.-C. Feng, K.-L. Chen, Y.-S. Li, H.-J. Deng, S.-M. Pan, D.-H. Wu, Y. Ding, CD36 inhibits β-catenin/c-myc-mediated glycolysis

through ubiquitination of GPC4 to repress colorectal tumorigenesis, Nat. Commun. 10 (1) (2019) 3981, https://doi.org/10.1038/s41467-019-11662-3.
[36] Y. Ma, L. Huang, Z. Zhang, P. Yang, Q. Chen, X. Zeng, F. Tan, C. Wang, X. Ruan, X. Liao, CD36 promotes tubular ferroptosis by regulating the ubiquitination of FSP1 in acute kidney injury, Genes Dis. 11 (1) (2024) 449–463, https://doi.org/10.1016/j.gendis.2022.12.003.
[37] R. Ehehalt, R. Sparia, H. Kulaksiz, T. Herrmann, J. Füllekrug, W. Stremme, Uptake of long chain fatty acids is regulated by dynamic interaction of FAT/CD36 with cholesterol/sphingolipid enriched microdomains (lipid rafts), BMC Cell Biol. 9 (2008) 45, https://doi.org/10.1186/1471-2121-9-45.
[38] J.-W. Park, W.-J. Park, Y. Kuperman, S. Boura-Halfon, Y. Pewzner-Jung, A. H. Futerman, Ablation of very long acyl chain sphingolipids causes hepatic insulin resistance in mice due to altered detergent-resistant membranes, Hepatology 57 (2) (2013) 525–532, https://doi.org/10.1002/hep.26015.
[39] E. Megha, London, Ceramide selectively displaces cholesterol from ordered lipid domains (rafts): implications for lipid raft structure and function, J. Biol. Chem. 279 (11) (2004) 9997–10004, https://doi.org/10.1074/jbc.m309992200.
[40] W.-J. Park, J.-W. Park, A.H. Merrill, J. Storch, Y. Pewzner-Jung, A.H. Futerman, Hepatic fatty acid uptake is regulated by the sphingolipid acyl chain length, Biochim Biophys Acta 1841 (12) (2014) 1754–1766, https://doi.org/10.1016/j.bbalip.2014.09.009.
[41] Y. Luan, H.R. Griffiths, Ceramides reduce CD36 cell surface expression and oxidised LDL uptake by monocytes and macrophages, Arch Biochem. Biophys. 450 (1) (2006) 89–99, https://doi.org/10.1016/j.abb.2006.03.016.